J. Fluid Mech. (1972), *vol.* 53, *part* 3, *pp.* 513–521
Printed in Great Britain

Flow of a stratified fluid in a wavy channel

By A. RAMACHANDRA RAO
AND RATHNA DEVANATHAN

Department of Applied Mathematics, Indian Institute of Science, Bangalore

(Received 13 December 1971)

The flow of a stratified fluid in a channel with small and large deformations is investigated. The analogy of this flow with swirling flow in tubes with non-uniform cross-sections is studied. The flow near the wall is blocked when the Froude number takes certain critical values. The possibility of preventing the stagnation zones in the flow field is also discussed.

1. Introduction

It has been observed that there exists an analogy between the flow of a stratified and a rotating fluid in many contexts. The important features of these flows are the blocking of the flow and the existence of internal waves for low Rossby and Froude numbers (Long 1953*a*, *b*; Trustrum 1964). Many such analogies have been discussed in great detail by Yih (1965).

The aim of the present investigation is to study the analogy between the dynamics of rotating fluids and those of stratified fluids in presence of wavy boundaries. Chow (1969) has studied the swirling flow in tubes with non-uniform cross-sections; it was found that the flow near the wall is blocked if the Rossby number takes some critical values depending upon the zeros of the Bessel function $J_1(\lambda)$. Further, for tubes with large periodic deformations, reversal of the flow was observed at the cross-sections of maximum and minimum area. The reverse-flow regions shift from one cross-section to the other when the Rossby number crosses the critical values. Such a backflow was also observed experimentally by Gore & Ranz (1964).

Recently Segur (1971) has examined the steady two-dimensional flow of a stratified fluid into an arbitrary contraction. The solution has been given when the strength of the contraction does not exceed a certain critical value depending on the Froude number.

In the work which follows, an attempt is made to understand the flow of a stratified fluid in a channel with small sinusoidal and large periodic wall deformations. In our analysis we take the governing nonlinear equations of motion, which reduce to a single equation for the stream function by choosing a suitable uniform upstream condition (Yih 1965). The solution for the stream function is obtained for two types of wall deformations, namely, (*a*) when the wall deformations are of out of phase and (*b*) when the wall deformations are in phase. The nature of the flow in case (*a*) is found to be analogous to the swirling flow in a tube with non-uniform cross-section, while the flow in case (*b*) exhibits different features.

Yih, O'Dell & Debler (1962) have explained the prevention of stagnation zones in the flow of a stratified fluid. This was achieved by introducing a structure near the sink, the form of which is obtained by making the mathematical singularity near the sink more complex. Is there any other approach for prevention of the stagnation zones which can be used instead of introducing an artificial mathematical singularity near the sink? In order to answer this our analysis has been extended to include the flow in a channel with large periodic wall deformations. The reversal of the flow and the separation zones are observed for small Froude numbers. We conclude that the stagnation zones in channel flow for small Froude numbers can be prevented by suitably deforming the walls of the channel. This appears to be a more natural way of preventing the stagnation zones than the method suggested by Yih *et al.* (1962).

2. Flow field in a channel with small sinusoidal deformations

Consider the steady two-dimensional flow of a non-homogeneous incompressible inviscid fluid in a channel with wavy walls. The co-ordinate axes x and y are chosen so that the undeformed walls are taken to be $y = \pm d$, where $2d$ is the distance between the walls. A transformation introduced by Yih (1965) is used to simplify the equations of motion. Writing

$$u' = (\rho/\rho_0)^{\frac{1}{2}} u, \quad v' = (\rho/\rho_0)^{\frac{1}{2}} v, \quad \psi' = \int (\rho/\rho_0)^{\frac{1}{2}} d\psi, \tag{1}$$

where ρ_0 is the reference density, u' and v' are the transformed velocities in the x and y directions and ψ' is the transformed stream function defined by

$$u' = \partial\psi'/\partial y, \quad v' = -\partial\psi'/\partial x,$$

the differential equation for ψ' is

$$\rho_0 \nabla^2 \psi' + gy \frac{d\rho}{d\psi'} = \frac{dH}{d\psi'}, \tag{2}$$

where
$$\nabla^2 \equiv \partial^2/\partial x^2 + \partial^2/\partial y^2,$$

$$H = p + \tfrac{1}{2}\rho(u^2+v^2) + \rho g y \tag{3}$$

and g is the gravitational acceleration.

The upstream density variation is taken to be linear and the upstream velocity is constant. Thus far upstream we have

$$u'_{-\infty} = u_0 = \text{constant}, \quad \rho_{-\infty} = \rho_0(1-\beta y), \tag{4}$$

where $\beta = (\rho_0 - \rho_1)/2d$, ρ_0 is the reference density, which is the density at the bottom of the channel ($y = -d$), and ρ_1 is the density at $y = d$. Hence we get

$$\left(\frac{d\rho}{d\psi'}\right)_{-\infty} = -\frac{\rho_0 \beta}{u_0}, \quad \left(\frac{dH}{d\psi'}\right)_{-\infty} = -\frac{\rho_0 \beta g}{u_0^2}\psi'_{-\infty}, \tag{5}$$

and (2) becomes

$$\nabla^2\psi' + \frac{g\beta}{u_0^2}\psi' = \frac{g\beta}{u_0}y. \tag{6}$$

The solution of (6) is investigated for two types of sinusoidal wall deformations.

(*a*) When the wall deformations are out of phase, the boundaries are

$$y = d + a\cos k'x \quad \text{and} \quad y = -d - a\cos k'x,$$

where a is the amplitude and k' is the wavenumber of the sinusoidal deformation.

(*b*) When the wall deformations are in phase, the boundaries are

$$y = d + a\cos k'x \quad \text{and} \quad y = -d + a\cos k'x.$$

Following Chow (1969), the condition that the flow is tangent to the wall becomes approximately

$$\left(\frac{v'}{u_0}\right)_{y=\pm d} = \frac{dy}{dx} \tag{7}$$

when $a/d \ll 1$.

Now, introducing the non-dimensional variables in the form

$$\left.\begin{aligned} U = u'/u_0, \quad V = v'/u_0, \quad \Psi = \psi'/u_0 d,\\ \xi = x/d, \quad \eta = y/d, \quad k' = k/d, \end{aligned}\right\} \tag{8}$$

equation (6) can be written as

$$\frac{\partial^2\Psi}{\partial\xi^2} + \frac{\partial^2\Psi}{\partial\eta^2} + F^{-2}\Psi = F^{-2}\eta, \tag{9}$$

where $F = u_0/d(g\beta)^{\frac{1}{2}}$ is the Froude number of the flow. The non-dimensional form of the boundary conditions in case (*a*) is given by

$$\left(\frac{\partial\Psi}{\partial\xi}\right)_{\eta=\pm1} = \pm\frac{a}{d}k\sin k\xi \tag{10}$$

and in case (*b*) by

$$\left(\frac{\partial\Psi}{\partial\xi}\right)_{\eta=\pm1} = \frac{a}{d}k\sin k\xi. \tag{11}$$

Taking the solution of (9) in the form

$$\Psi = \eta + f(\eta)\cos k\xi, \tag{12}$$

the differential equation for $f(\eta)$ becomes

$$d^2f/d\eta^2 + (F^{-2} - k^2)f = 0. \tag{13}$$

Equation (13) gives three possible solutions depending on the magnitude of $(F^{-2} - k^2)$. The solutions for the stream function and the axial velocity satisfying the boundary conditions in case (a) are given by

$$\left.\begin{aligned} \Psi &= \eta-\frac{a}{d}\frac{\sin(F^{-2}-k^2)^{\frac{1}{2}}\eta}{\sin(F^{-2}-k^2)^{\frac{1}{2}}}\cos k\xi, &(14)\\ U &= 1-\frac{a}{d}\frac{(F^{-2}-k^2)^{\frac{1}{2}}\cos(F^{-2}-k^2)\eta}{\sin(F^{-2}-k^2)}\cos k\xi, &(15)\end{aligned}\right\}\quad \text{when}\quad F^{-2}>k^2,$$

$$\left.\begin{aligned} \Psi &= \eta-\frac{a}{d}\eta\cos k\xi, &(16)\\ U &= 1-\frac{a}{d}\cos k\xi, &(17)\end{aligned}\right\}\quad \text{when}\quad F^{-2}=k^2,$$

$$\left.\begin{aligned} \Psi &= \eta-\frac{a}{d}\frac{\sinh(k^2-F^{-2})^{\frac{1}{2}}\eta}{\sinh(k^2-F^{-2})^{\frac{1}{2}}}\cos k\xi, &(18)\\ U &= 1-\frac{a}{d}\frac{(k^2-F^{-2})^{\frac{1}{2}}\cosh(k^2-F^{-2})^{\frac{1}{2}}\eta}{\sinh(k^2-F^{-2})^{\frac{1}{2}}}\cos k\xi, &(19)\end{aligned}\right\}\quad \text{when}\quad F^{-2}<k^2$$

and in the case (b) by

$$\left.\begin{aligned} \Psi &= \eta+\frac{a}{d}\frac{\cos(F^{-2}-k^2)^{\frac{1}{2}}\eta}{\cos(F^{-2}-k^2)^{\frac{1}{2}}}\cos k\xi, &(20)\\ U &= 1-\frac{a}{d}\frac{(F^{-2}-k^2)^{\frac{1}{2}}\sin(F^{-2}-k^2)^{\frac{1}{2}}\eta}{\cos(F^{-2}-k^2)^{\frac{1}{2}}}\cos k\xi, &(21)\end{aligned}\right\}\quad \text{when}\quad F^{-2}>k^2,$$

$$\left.\begin{aligned} \Psi &= \eta+\frac{a}{d}\eta\cos k\xi, &(22)\\ U &= 1+\frac{a}{d}\cos k\xi, &(23)\end{aligned}\right\}\quad \text{when}\quad F^{-2}=k^2,$$

$$\left.\begin{aligned} \Psi &= \eta+\frac{a}{d}\frac{\cosh(k^2-F^{-2})^{\frac{1}{2}}\eta}{\cosh(k^2-F^{-2})^{\frac{1}{2}}}\cos k\xi, &(24)\\ U &= 1+\frac{a}{d}\frac{(k^2-F^{-2})^{\frac{1}{2}}\sinh(k^2-F^{-2})^{\frac{1}{2}}\eta}{\cosh(k^2-F^{-2})^{\frac{1}{2}}}\cos k\xi, &(25)\end{aligned}\right\}\quad \text{when}\quad F^{-2}<k^2.$$

It is evident that the results (14) and (15) are not valid when the parameter $(F^{-2}-k^2)^{\frac{1}{2}}$ takes the values $n\pi$ $(n = 1, 2, 3, \ldots)$, similarly, the results (20) and (21) are not valid when this parameter takes the values $\frac{1}{2}(2n+1)\pi$ $(n = 0, 1, 2, \ldots)$. Thus there exist infinitely many critical Froude numbers

$$F_{cr} = (n^2\pi^2+k^2)^{-\frac{1}{2}} \quad (n = 1, 2, \ldots) \quad \text{for} \quad \text{case } (a), \tag{26}$$

$$F_{cr} = [\tfrac{1}{4}(2n+1)^2\pi^2+k^2]^{-\frac{1}{2}} \quad (n = 0, 1, \ldots) \quad \text{for} \quad \text{case } (b); \tag{27}$$

at these critical values of the Froude numbers no solution of (6) can be found to satisfy the boundary condition (7). The physical explanation of this situation is that the fluid cannot go round the bumps in the wall steadily and forms a stagnant region there. This is called the phenomenon of blocking and occurs in the flow of stratified fluids discussed in detail by Yih (1965) and others (see Segur 1971; Drazin 1961; Debler 1959).

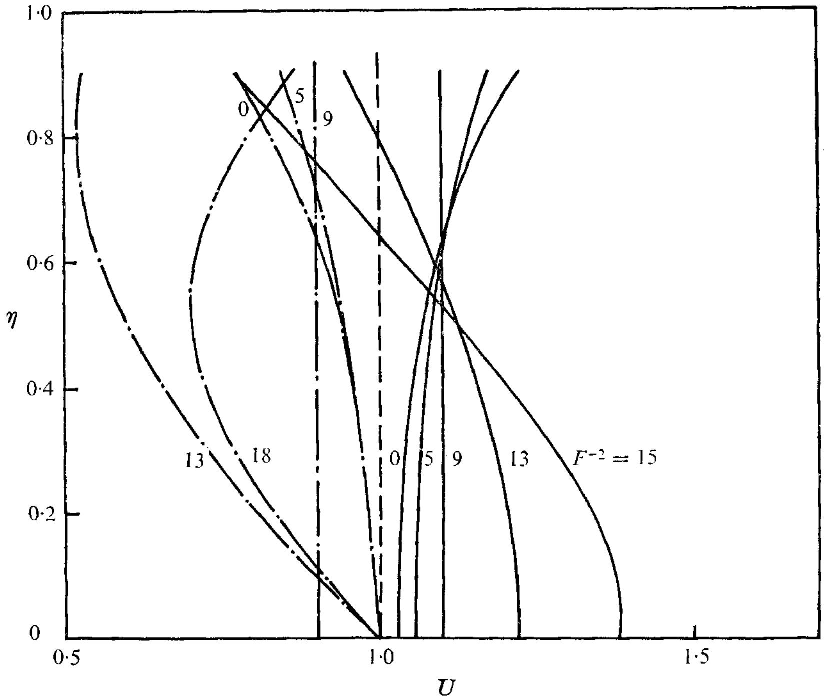

FIGURE 1. Axial velocity across $k\xi = \pi$ for small Froude numbers with $k = 3$ and $a/d = 0{\cdot}1$. ——, case (*a*), — - —, case (*b*).

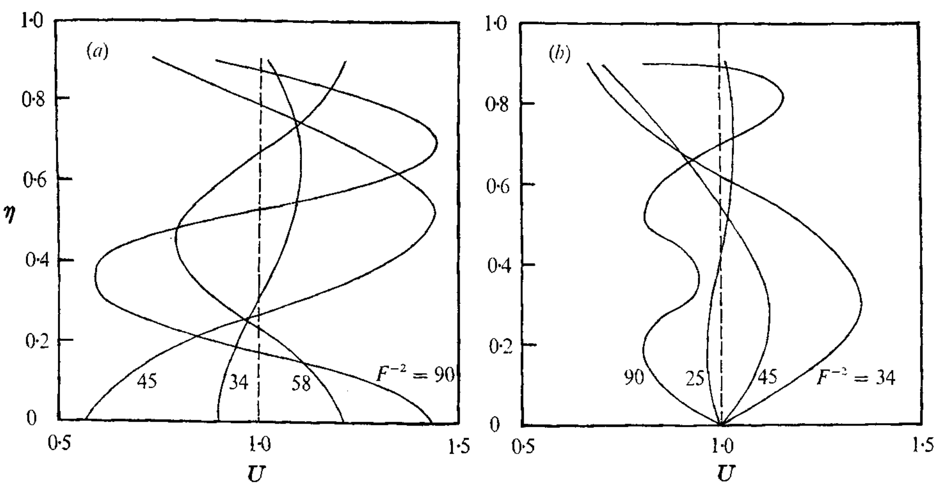

FIGURE 2. Axial velocity across $k\xi = \pi$ for very small Froude numbers with $k = 3$ and $a/d = 0{\cdot}02$. (*a*) Case (*a*). (*b*) Case (*b*).

The axial velocity at the cross-section $k\xi = \pi$ is shown in figures 1 and 2 for different Froude numbers. It is seen from figure 1 that for case (*a*) decreasing the Froude number accelerates the flow in the mid-plane and decelerates the flow near the boundary. On the other hand, when the Froude number passes

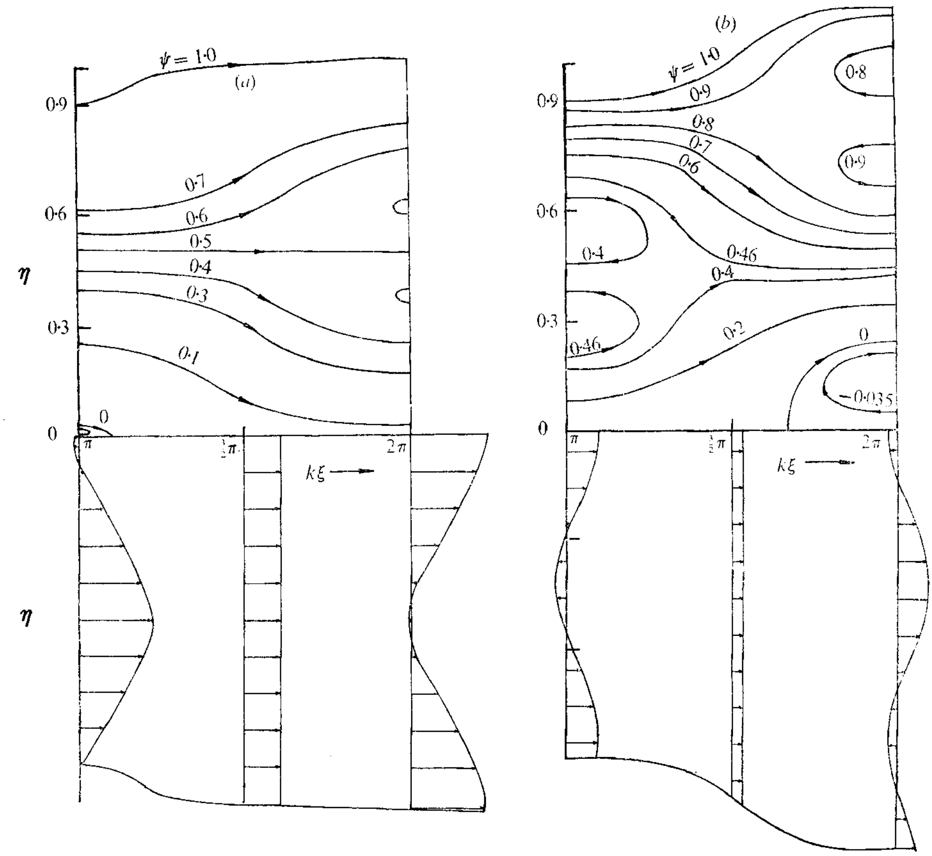

FIGURE 3. Streamlines and axial velocity profiles for case (i). (a) $F^{-2} = 48$, $k = 3$ and $c_1 = 0{\cdot}166$. (b) $F^{-2} = 64$, $k = 3$ and $c_1 = 0{\cdot}280$.

the first critical value, as given in (26), the flow decelerates in the mid-plane, accelerates in the outer region and decelerates near the boundary (figure 2). Similarly, when the Froude number passes the higher critical values some changes in the flow will again take place.

In case (b), the flow in the mid-plane is neither accelerated nor decelerated but remains uniform for all Froude numbers, except for $F^{-2} = 9$, when the flow is uniform throughout. It is observed that the flow always decelerates near the boundary, while in the outer region it is accelerated for some Froude numbers and decelerated for other Froude numbers. For very small Froude numbers the flow in the outer region is quite complicated.

3. Flow field in a channel with large periodic wall deformations

For large periodic wall deformations the shape of the wall is not specified *a priori*. Using the two exact solutions derived in § 2 one can study the behaviour of the stratified flow in channels with large periodic wall deformations by an

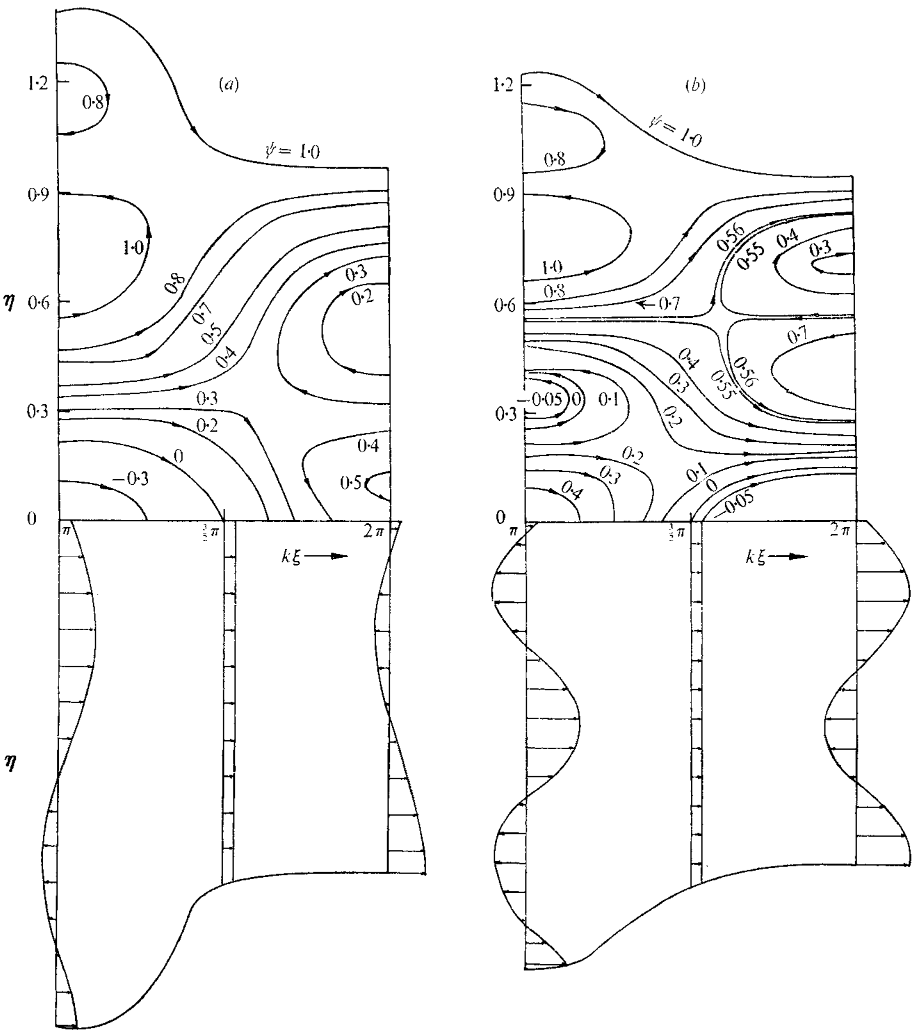

FIGURE 4. Streamlines and axial velocity profiles for case (ii). (*a*) $F^{-2} = 34$, $k = 3$ and $c_2 = 0{\cdot}474$, (*b*) $F^{-2} = 81$, $k = 3$ and $c_2 = -0{\cdot}470$.

inverse method. Consider

$$\text{(i)} \quad \Psi = \eta + c_1 \sin (F^{-2} - k^2)^{\frac{1}{2}} \eta \cos k\xi, \tag{28}$$

$$\text{(ii)} \quad \Psi = \eta + c_2 \cos (F^{-2} - k^2)^{\frac{1}{2}} \eta \cos k\xi, \tag{29}$$

which are exact solutions of (9). The shape of the boundary is controlled by the arbitrary constants c_1 and c_2, which need not be very small. The streamlines and the axial velocity profiles are represented graphically in the region $\pi \leqslant k\xi \leqslant 2\pi$ for cases (i) and (ii) by determining the arbitrary constants c_1 and c_2 such that $\Psi = 1$ and $\eta = 0{\cdot}9$ when $k\xi = \pi$.

The streamlines and the axial velocity profiles for case (i) are shown in figure 3. Even for moderately small Froude numbers, reversed flow exists at both the

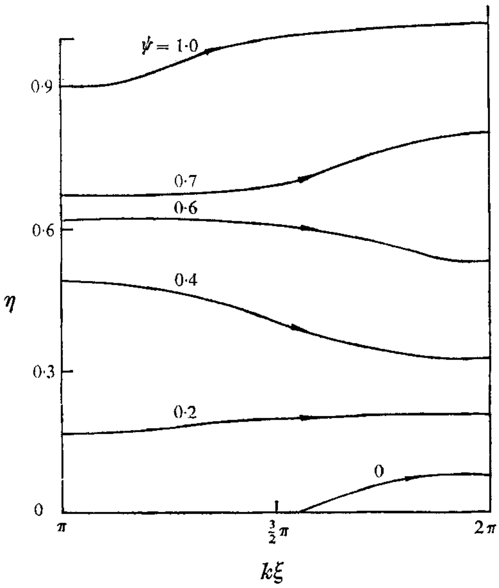

FIGURE 5. Streamlines at $F^{-2} = 64$ with $k = 3$ and $c_2 = -0{\cdot}108$ for case (ii).

cross-sections of maximum and minimum area. These Froude numbers are chosen to lie in between the second and third critical values. It is seen from the figures that the nature of the axial velocity in the central plane changes as the Froude number crosses the critical values. However, for slight differences, the general structure of this separated flow region is analogous to the swirling flow in tubes with non-uniform cross-sections (Chow 1969).

Figure 4 depicts the streamlines and the axial velocity profiles for case (ii). Here also the backflow regions are observed at both the cross-sections of maximum and minimum area. The flow pattern becomes quite complicated in structure for very small Froude numbers as shown in figure 4 (*b*). Another striking feature which we notice from our calculations is that even for the same small Froude number no reversed flow takes place for case (i). The reason for this type of behaviour is that the critical Froude numbers are different for cases (i) and (ii).

By analysing the streamline patterns and axial velocity profiles for various Froude numbers for cases (i) and (ii), it is concluded that the separation-flow regions which occur in one case for a particular Froude number can be prevented in the other case. In other words, the stagnation zones in channel flow for very small Froude numbers can be prevented by suitably deforming the walls of the channel. As an example, figure 3 (*b*) (case (i)) shows the presence of separated-flow regions for $F^{-2} = 64$, while figure 5 (case (ii)) shows that there is no reversed flow for the same Froude number. However, these theoretical predictions are yet to be supported by experiments.

REFERENCES

Chow, C. Y. 1969 *J. Fluid Mech.* **38**, 843.

Debler, W. R. 1959 *Proc. A.S.C.E.* **85**, 51.

Drazin, P. G. 1961 *Tellus*, **13**, 239.

Gore, R. W. & Ranz, W. E. 1964 *A.I.Ch.E. J.* **10**, 83.

Long, R. R. 1953*a* *Tellus*, **5**, 42.

Long, R. R. 1953*b* *J. Meteor.* **10**, 197.

Segur, H. 1971 *J. Fluid Mech.* **48**, 161.

Trustrum, K. 1964 *J. Fluid Mech.* **19**, 415.

Yih, C.-S. 1965 *Dynamics of Nonhomogeneous Fluids*. Macmillan.

Yih, C.-S., O'Dell, W. & Debler, W. R. 1962 *Proc. 4th U.S. Nat. Congr. Appl. Mech.* p. 1441.